Experimental Study of Slow-Rate Transition Crossing in AGS *

J. Wei, A. Warner, L. Ahrens, J.M. Brennan, W.W. MacKay, S. Peggs, A. Ratti, K. Reece,
T. Roser, W.A. Ryan, C. Saltmarsh, T. Satogata, D. Trbojevic, W. Van Asselt
Brookhaven National Laboratory
Upton, New York 11973, USA

Abstract

The nonlinear momentum-compaction factor α_1 has been obtained in the AGS by measuring transition energies at different radial orbits using a low-intensity slow-ramped Au^{77+} beam. The beam loss during the transition crossing is found to increase with increasing rf voltage, and to decrease with increasing ramping rate, which indicates that the effect of chromatic nonlinearity (Jøhnsen effect) dominates the transition crossing. The experimental measurement of beam loss agrees very well with TIBETAN computer simulation.

1 INTRODUCTION

During the past several decades, the crossing of transition energy has been of primary concern in the design of hadron accelerators. In the recently proposed machines like the Relativistic Heavy Ion Collider (RHIC), particles are accelerated through transition at a relatively slow rate due to the slow ramping rate of the superconducting magnets. Effects of chromatic nonlinearities (the Jøhnsen Effect[1]) often become significant.

The nonlinear momentum-compaction factor α_1 which partly produces chromatic nonlinear effects has previously been determined for the ISR by measuring the nonlinear change in revolution frequency, and also for the SPS by a transition timing measurement.[2] The purpose of this study is first to experimentally deduce the α_1 factor in the AGS, and then to verify the Jøhnsen-effect theory by comparing the experimental results with computer simulation on beam loss as a function of rf voltage V, crossing rate $\dot{B}$, and the time of synchronous-phase switch-over.

The experiment was performed in the AGS in November 1993. In order to minimize multiparticle effects, we used low intensity Au^{77+} beam crossing transition at slow acceleration rates. The transition energy is determined by measuring the time of the phase switch-over at which the beam loss through transition is the minimum. The α_1 factor is obtained by measuring the variation in transition energy as a function of beam mean radial orbit, which corresponds to a momentum offset. In Section 2, we present the theory pertaining to chromatic nonlinearities. Experimental setup and data reduction methods are summarized in Section 3. The α_1 factor is obtained in Section 4 under various sextupole-current settings. Comparison is given in Section 5 on beam loss between experimental results and computer simulation. The conclusion is given in Section 6.

2 EFFECTS OF CHROMATIC NONLINEARITIES

In the low-intensity limit when the multiparticle effects are negligible, the longitudinal motion of the particle can be described in terms of its rf phase ϕ and energy deviation $W \equiv \Delta E / h\omega_s$ by the equations

$$
\begin{cases}
W_{n+1} = W_n + \dfrac{qeV}{h\omega_s}(\sin\phi_n - \sin\phi_{s,n}) \\
\phi_{n+1} = \phi_n + \dfrac{2\pi h^2 \omega_s \eta(W_{n+1})}{E_s\beta_s} W_{n+1} + \phi_{s,n+1} - \phi_{s,n}
\end{cases}
\tag{1}
$$

where ϕ_s, ω_s, $\beta_s c$, E_s are the synchronous phase, revolution frequency, velocity, and energy, respectively, and h and V are the rf harmonic and voltage. Here the slip factor

$$
\eta(W) \approx \alpha_0 - \frac{1}{\gamma_s^2} + \alpha_0\left(\alpha_1 + \frac{3}{2}\beta_s^2\right)\delta
\tag{2}
$$

depends on the zeroth ($\alpha_0 \equiv 1/\gamma_{t0}^2$) and first ($\alpha_1$) order momentum-compaction factor, where $\delta = h\omega_s W/E\beta_s^2$ is the momentum deviation. Due to the nonlinearity in the machine lattice and the particle motion, particles of different momenta δ cross transition at different times

$$
\beta_s^2 \dot{B} \Delta t = -\left(\alpha_1 + \frac{3}{2}\beta_s^2\right)B\delta
\tag{3}
$$

where B and $\dot{B}$ are the magnetic field and ramping rate.

Based on Eq. 3, the first part of the experiment was designed to measure the nonlinear momentum-compaction factor α_1 in the AGS using a low-intensity Au^{77+} beam. The beam was made to cross transition at orbits of different momenta (δ) under the same machine conditions ($\dot{B}$, B, β_s, etc.). The variation Δt in the time of transition crossing was determined by measuring at the various radial orbits the time of synchronous-phase switch-over that results in the minimum beam loss.

The second part of the experiment consisted of measuring the beam loss as functions of phase-switch delay time, rf voltage V, and ramping rate $\dot{B}$. With the factor α_1 and the bunch area evaluated from the experimental data, comparison can be made with theoretical estimates and computer simulations. Theoretically, longitudinal emittance growth caused by the chromatic nonlinearities (the Jøhnsen effect) is proportional to the ratio T_{nl}/T_C of the nonlinear time T_{nl} to the characteristic transition time T_C, where

$$
T_C = \left(\frac{\pi E\beta_s^2\gamma_T^3}{qeV|\cos\phi_s|\dot{\gamma}_s h\omega_s^2}\right)^{\frac{1}{3}}, \quad T_{nl} = \frac{\left|(\alpha_1 + \frac{3}{2}\beta_s^2)\right|\delta(0)\gamma_{t0}}{\dot{\gamma}_s},
\tag{4}
$$

976

and $\hat{\delta}(0)$ is the maximum momentum spread at transition. Beam loss occurs when the particle escapes the rf bucket and, when the momentum exceeds the aperture.

3 EXPERIMENTAL SETUP AND DATA REDUCTION

We perform the experiment in the AGS with Au^{77+} beams at an intensity of about 1×10^8 ions per bunch. The beam was made to cross transition ($\gamma_{t0} \approx 8.3$) at various rates $\dot{B}=0.05, 0.1$, and 0.5 T/s. The longitudinal bunch profiles measured through the wall current monitor were recorded at 5 ms time intervals on a LeCroy 7200 digital oscilloscope with 1 ns sampling resolution triggered by the gauss-clock event which corresponds to a specified B field. The recorded data (Fig. 1) was then transferred into SDS (Self-
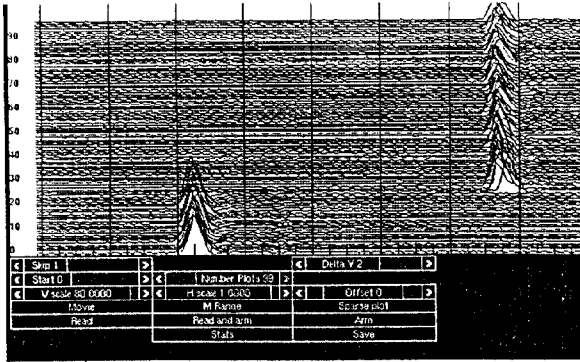
Figure 1: Typical digitized beam-profile data.

Describing Structure) format along with various beam and machine parameters, including beam intensity, V, B, $\dot{B}$, γ_t, and the trigger delay time.

Signal deterioration due to system bandwidth limitation and cable attenuation was determined by analyzing the signals on the LeCroy scope generated by a series of pulses of various time duration, inserted at the wall-current monitor terminal. For pulses of FWHM width (W_s) from 2 to 15ns, the measured width W_m is broadened by about 1.9 ns,

$$W_m = 1.03 \, W_s + 1.9 \quad \text{(ns)}. \qquad (5)$$

The corresponding correction is made to the measured data during the analysis.

A computer program GT_ANALY has been developed to analyse the SDS format beam-profile data generated either from the LeCroy scope or TIBETAN computer simulation.[3] GT_ANALY first evaluates the average background level using χ^2 fitting. After the background is subtracted, the beam intensity, rms bunch length, skewness, and kurtosis are subsequently evaluated by numerical integrations. The longitudinal beam emittance is calculated from the obtained bunch length using the calibrated rf voltage, magnetic field, and other machine parameters. The beam loss is determined by evaluating the difference in beam intensity at times (typically 100 ms) before and after the transition phase jump, which are long compared with T_C (typically 10 ms).

The accuracy of the beam emittance calculation depends on the calibration of the average magnetic field, the rf voltage, and the pulse broadening. The magnetic field is obtained from the gauss-clock reading which has been calibrated by the frequency measurement. The rf voltage is calibrated at various ramping rates ($\dot{B}=0.05, 0.1$, and 0.5 T/s) by evaluating, at various voltage settings from 20 to 270 kV, the actual rf voltage applied on the beam, which is deduced from the amount of synchronous phase jump at transition.

4 MEASUREMENT OF α_1 FACTOR

Measurement of the nonlinear momentum-compaction factor α_1 is performed under three sextupole current (I_H, I_V) settings at (190 A,0), (0,200 A), and (0,0), respectively. At each sextupole setting, the beam is made to cross transition at two different radial orbits. As shown in Fig. 2, the time of synchronous-phase switch-over near transi-
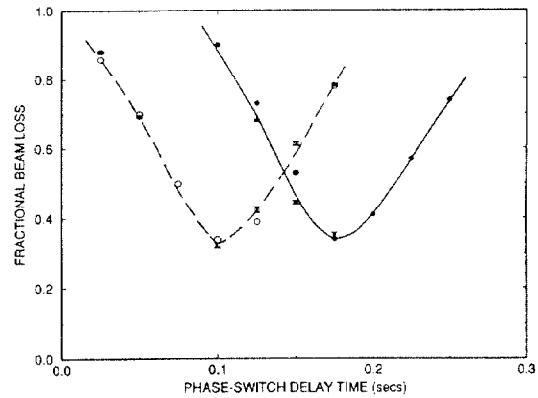
Figure 2: Beam loss versus the phase-switch delay time at radial positions $V_R = 3.0$ V (left) and 2.5 V (right), respectively, at $\dot{B} = 0.1$ T/s with $(I_H, I_V) = (190$ A,0$)$.

tion is varied at two radial-loop settings. The times for the beam center to cross the transition energy correspond to the times of the minimum beam loss. The difference $\Delta t \approx (-72\pm7)$ ms in the minimum-loss delay time between these two orbits corresponds to the difference in transition energy at these two momentum offsets.

In order to determine the factor α_1 using Eq. 3, the momentum offset δ is calibrated against the radial-loop setting V_R using the frequency measurement. The measurement is performed at energy $\gamma = 12.0$ far above the transition energy. The relation obtained is

$$\delta/\Delta V_R = (4.8 \pm 0.2) \times 10^{-3} \text{ V}^{-1}. \qquad (6)$$

This result is consistent with the Ionization Position Monitor (IPM) measurement of the beam radial centroid position at different radial-loop settings using a dispersion of 3.2 meters at the IPM location.

Using Eq. 6, the factor α_1 has been obtained along with the transition energy γ_{t0} at the various sextupole settings. The results are summarized in Table 1.

5 COMPARISON OF EXPERIMENTAL AND SIMULATION RESULTS

With γ_{t0} and α_1 given in Table 1, and with the initial longitudinal emittance evaluated by GT_ANALY, computer simulation is performed to verify the experimental measurement on beam loss as functions of the phase-switch time, rf voltage V, and ramping rate $\dot{B}$. The simulation is performed with 2000 test particles using the computer program TIBETAN based on Eq. 1. The solid line in Fig. 3 shows the simulated beam loss versus switch-over time,
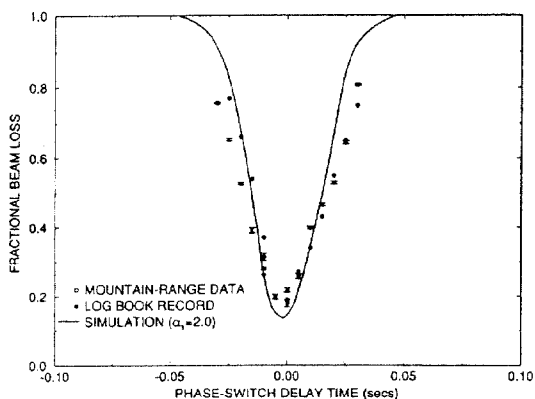

Figure 3: Beam loss versus the synchronous-phase switch-over time at $\dot{B}$ =0.5 T/s.

which agrees well with the experimental results of both the GT_ANALY beam-profile analysis and the beam current transformer readings (log book record).

At a fixed ramping rate $\dot{B}$, an increase in rf voltage causes an increase in bunch momentum spread, thus enhancing the effect of chromatic nonlinearities. Fig. 4 shows the beam loss versus the voltage V obtained from the log book record, beam-profile analysis, and simulation. At voltages below 35 kV, the beam does not survive due to the vanishing rf bucket.

At a fixed rf voltage V, a decrease in the ramping rate $\dot{B}$ causes an increase in the nonlinear time T_{nl}, thus enhancing the nonlinear effect, as shown by the experimental data points in Fig. 5. The solid curve shows the result of computer simulation using the initial emittance evaluated from the beam profiles. The measured FWHM's of the signals are 15.5, 5.7, and 4.5 ns at $\dot{B}$ = 0.5, 0.1, and 0.05 T/s, respectively. The bandwidth correction becomes significant for the low $\dot{B}$ cases when the beam width is comparable to the bandwidth broadening (1.9 ns).

6 CONCLUSION

The AGS momentum-compaction factor was obtained up to the first nonlinear order by measuring the variation of

Table 1: AGS Transition energy and α_1 at V_R = 3.0 V.

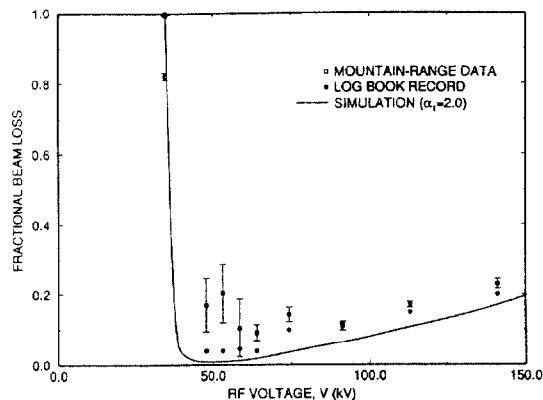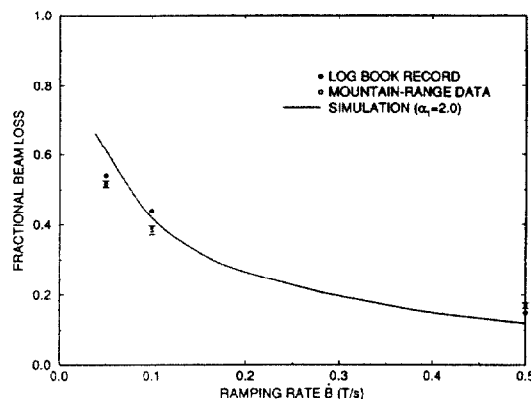| (I_H, I_V) (A)	(190, 0)	(0, 200)	(0, 0)
γ_{t0}	8.28	8.34	8.31
α_1	2.1±0.5	4.5±0.9	5.4±1.0

Figure 4: Beam loss versus rf voltage at $\dot{B}$ =0.5 T/s.

Figure 5: Beam loss versus crossing rate $\dot{B}$ at V =114 kV.

transition energy with radial orbit using a low-intensity slow-ramped Au^{77+} beam. The α_1 value varies from 2.0 to 5.4 under the various sextupole-current settings.

In the case of low beam intensity and slow ramping rate, the effect of chromatic nonlinearity dominates the transition crossing. The beam loss during transition crossing is found to generally increase with increasing rf voltage, and to decrease with increasing ramping rate. Computer simulation has been performed using the experimentally obtained factors α_1, γ_{t0}, and initial beam emittance. The agreement between the experimental measurement and computer simulation is good within experimental accuracy.

7 REFERENCES

[1] K. Jøhnsen, Proc. CERN Symp. High-Energy Accel. and Pion Physics (Geneva, 1956), Vol.1, p.106; K. Takayama, Part. Accel. 14, 201 (1984); S.Y. Lee and J. Wei, EPAC Proc. (Rome, 1988), p.764.

[2] E. Ciapala, etc. IEEE Trans. Nucl. Sci. **NS-26**, 3571 (1979); P. Faugeras, etc. IEEE Trans. Nucl. Sci. **NS-26**, 3577 (1979).

[3] J. Wei, *Longitudinal Dynamics of the Non-Adiabatic Regime on Alternating-Gradient Synchrotrons*, Ph.D thesis, SUNY at Stony Brook, 1990; J. Wei, etc. these proceedings.